Nonlinear phase noise mitigation in phase-sensitive amplified transmission systems

Citation for the original published paper (version of record):
Olsson, S., Karlsson, M., Andrekson, P. (2015). Nonlinear phase noise mitigation in phase-sensitive amplified transmission systems. Optics Express, 23(9): 11724-11740.
http://dx.doi.org/10.1364/OE.23.011724

Nonlinear phase noise mitigation in phase-sensitive amplified transmission systems

Samuel L.I. Olsson,* Magnus Karlsson, and Peter A. Andrekson

Photonics Laboratory, Department of Microtechnology and Nanoscience, Chalmers University of Technology, SE-412 96, Gothenburg, Sweden

*samuel.olsson@chalmers.se

Abstract: We investigate the impact of in-line amplifier noise in transmission systems amplified by two-mode phase-sensitive amplifiers (PSAs) and present the first experimental demonstration of nonlinear phase noise (NLPN) mitigation in a modulation format independent PSA-amplified transmission system. The NLPN mitigation capability is attributed to the correlated noise on the signal and idler waves at the input of the transmission span. We study a single-span system with noise loading in the transmitter but the results are expected to be applicable also in multi-span systems. The experimental investigation is supported by numerical simulations showing excellent agreement with the experiments. In addition to demonstrating NLPN mitigation we also present a record high sensitivity receiver, enabled by low-noise PSA-amplification, requiring only 4.1 photons per bit to obtain a bit error ratio (BER) of 1×10^{-3} with 10 GBd quadrature phase-shift keying (QPSK) data.

OCIS codes: (060.2320) Fiber optics amplifiers and oscillators; (190.4380) Nonlinear optics, four-wave mixing.

References and links

1. C. M. Caves, "Quantum limits on noise in linear amplifiers," Phys. Rev. D **26**, 1817–1839 (1982).
2. Z. Tong, C. Lundström, P. A. Andrekson, C. J. McKinstrie, M. Karlsson, D. J. Blessing, E. Tipsuwannakul, B. J. Puttnam, H. Toda, and L. Grüner-Nielsen, "Towards ultrasensitive optical links enabled by low-noise phase-sensitive amplifiers," Nature Photon. **5**, 430–436 (2011).
3. S. L. I. Olsson, B. Corcoran, C. Lundström, M. Sjödin, M. Karlsson, and P. A. Andrekson, "Phase-sensitive amplified optical link operating in the nonlinear transmission regime," in *European Conference and Exhibition on Optical Communication (ECOC)* Paper Th.2.F.1, 2012.
4. S. L. I. Olsson, B. Corcoran, C. Lundström, T. A. Eriksson, M. Karlsson, and P. A. Andrekson, "Phase-sensitive amplified transmission links for improved sensitivity and nonlinearity tolerance," J. Lightw. Technol. (2014).
5. R.-J. Essiambre, G. Kramer, P. J. Winzer, G. J. Foschini, and B. Goebel, "Capacity limits of optical fiber networks," J. Lightw. Technol. **28**, 662–701 (2010).
6. A. D. Ellis, J. Zhao, and D. Cotter, "Approaching the non-linear Shannon limit," J. Lightw. Technol. **28**, 423–433 (2010).
7. E. Agrell, "Nonlinear fiber capacity," in *European Conference and Exhibition on Optical Communication (ECOC)* Paper We.4.D.8, 2013.
8. S. L. I. Olsson, C. Lundström, M. Karlsson, and P. A. Andrekson, "Long-haul (3465 km) transmission of a 10 GBd QPSK signal with low noise phase-sensitive in-line amplification," in *European Conference and Exhibition on Optical Communication (ECOC)* Paper PD.2.2, 2014.
9. R. Slavík, F. Parmigiani, J. Kakande, C. Lundström, M. Sjödin, P. A. Andrekson, R. Weerasuriya, S. Sygletos, A. D. Ellis, L. Grüner-Nielsen, D. Jakobsen, S. Herstrøm, R. Phelan, J. O'Gorman, A. Bogris, D. Syvridis, S. Dasgupta, P. Petropoulos, and D. J. Richardson, "All-optical phase and amplitude regenerator for next-generation telecommunications systems," Nature Photon. **4**, 690–695 (2010).

#235784 - $15.00 USD Received 6 Mar 2015; revised 15 Apr 2015; accepted 16 Apr 2015; published 24 Apr 2015

10. Z. Tong, C. Lundström, P. A. Andrekson, M. Karlsson, and A. Bogris, "Ultralow noise, broadband phase-sensitive optical amplifiers, and their applications," IEEE J. Sel. Topics Quantum Electron. **18**, 1016–1032 (2012).
11. T. Umeki, M. Asobe, H. Takara, Y. Miyamoto, and H. Takenouchi, "Multi-span transmission using phase and amplitude regeneration in PPLN-based PSA," Opt. Express **21**, 18170–18177 (2013).
12. T. Umeki, O. Tadanaga, M. Asobe, Y. Miyamoto, and H. Takenouchi, "First demonstration of high-order QAM signal amplification in PPLN-based phase sensitive amplifier," Opt. Express **22**, 2473–2482 (2014).
13. Z. Tong and S. Radic, "Low-noise optical amplification and signal processing in parametric devices," Advances in Optics and Photonics **5**, 318–384 (2013).
14. Z. Tong, C. J. McKinstrie, C. Lundström, M. Karlsson, and P. A. Andrekson, "Noise performance of optical fiber transmission links that use non-degenerate cascaded phasesensitive amplifiers," Opt. Express **18**, 15426–15439 (2010).
15. J. P. Gordon and L. F. Mollenauer, "Phase noise in photonic communications systems using linear amplifiers," Opt. Lett. **15**, 1351–1353 (1990).
16. B. Corcoran, S. L. I. Olsson, C. Lundström, M. Karlsson, and P. A. Andrekson, "Mitigation of nonlinear impairments on QPSK data in phase-sensitive amplified links," in *European Conference and Exhibition on Optical Communication (ECOC)* Paper We.3.A.1, 2013.
17. A. Bononi, P. Serena, and N. Rossi, "Nonlinear signal-noise interactions in dispersion-managed links with various modulation formats," Optical Fiber Technology **16**, 73–85 (2010).
18. Z. Tong, A. Bogris, C. Lundström, C. J. McKinstrie, M. Vasilyev, M. Karlsson, and P. A. Andrekson, "Modeling and measurement of the noise figure of a cascaded non-degenerate phase-sensitive parametric amplifier," Opt. Express **18**, 14820–14835 (2010).
19. C. J. McKinstrie, S. Radic, and M. G. Raymer, "Quantum noise properties of parametric amplifiers driven by two pump waves," Opt. Express **12**, 5037–5066 (2004).
20. B. Corcoran, R. Malik, S. L. I. Olsson, C. Lundström, M. Karlsson, and P. A. Andrekson, "Noise beating in hybrid phase-sensitive amplifier systems," Opt. Express **22**, 5762–5771 (2014).
21. R. Malik, A. Kumpera, S. L. I. Olsson, P. A. Andrekson, and M. Karlsson, "Optical signal to noise ratio improvement through unbalanced noise beating in phase-sensitive parametric amplifiers," Opt. Express **22**, 10477–10486 (2014).
22. K.-P. Ho, "Probability density of nonlinear phase noise," J. Opt. Soc. Am. B **20**, 1875–1879 (2003).
23. S. L. I. Olsson, B. Corcoran, C. Lundström, E. Tipsuwannakul, S. Sygletos, A. D. Ellis, Z. Tong, M. Karlsson, and P. A. Andrekson, "Injection locking-based pump recovery for phase-sensitive amplified links," Opt. Express **21**, 14512–14529 (2013).
24. C. Lundström, R. Malik, L. Grüner-Nielsen, B. Corcoran, S. L. I. Olsson, M. Karlsson, and P. A. Andrekson, "Fiber optic parametric amplifier with 10-dB net gain without pump dithering," IEEE Photon. Technol. Lett. **25**, 234–237 (2013).
25. K. Kikuchi and S. Tsukamoto, "Evaluation of sensitivity of the digital coherent receiver," J. Lightw. Technol. **26**, 1817–1822 (2008).
26. X. Liu, A. R. Chraplyvy, P. J. Winzer, R. W. Tkach, and S. Chandrasekhar, "Phase-conjugated twin waves for communication beyond the Kerr nonlinearity limit," Nature Photon. **7**, 560–568 (2013).
27. Y. Tian, Y.-K. Huang, S. Zhang, P. R. Prucnal, and T. Wang, "Demonstration of digital phase-sensitive boosting to extend signal reach for long-haul WDM systems using optical phase-conjugated copy," Opt. Express **21**, 5099–5106 (2013).
28. R. A. Fisher, B. R. Suydam, and D. Yevick, "Optical phase conjugation for time-domain undoing of dispersive self-phase-modulation effects," Opt. Lett. **8**, 611–613 (1983).
29. P. Minzioni, "Nonlinearity compensation in a fiber-optic link by optical phase conjugation," Fiber and Integrated Optics **28**, 179–209 (2009).
30. H. Hu, R. M. Jopson, A. H. Gnauck, M. Dinu, S. Chandrasekhar, X. Liu, C. Xie, M. Montoliu, S. Randel, and C. J. McKinstrie, "Fiber nonlinearity compensation of an 8-channel WDM PDM-QPSK signal using multiple phase conjugations," in *Optical Fiber Communication Conference and Exposition (OFC)* Paper M3C.2, 2014.
31. E. Ip and J. M. Kahn, "Compensation of dispersion and nonlinear impairments using digital backpropagation," J. Lightw. Technol. **26**, 3416–3425 (2008).
32. N. Alic, E. Myslivets, E. Temprana, B. P.-P. Kuo, and S. Radic, "Nonlinearity cancellation in fiber optic links based on frequency referenced carriers," J. Lightw. Technol. **32**, 2690–2698 (2014).

1. Introduction

It is well-known that phase-sensitive amplifiers (PSAs) can provide low-noise optical amplification [1, 2], and recently it was shown that they can also mitigate nonlinear transmission distortions in a modulation format independent scheme [3, 4]. The reach and channel capacity of fiber optical communication systems is limited by signal degradation due to amplifier

#235784 - $15.00 USD Received 6 Mar 2015; revised 15 Apr 2015; accepted 16 Apr 2015; published 24 Apr 2015

noise and fiber nonlinearities [5–7]. Using PSAs it should therefore be possible to obtain improved transmission reach compared to using conventional phase-insensitive amplifiers (PIAs). This was recently experimentally demonstrated in a multi-span transmission system where a threefold reach improvement was obtained using in-line PSAs compared to using conventional erbium-doped fiber amplifiers (EDFAs) at optimal launch power, due to low-noise amplification and nonlinearity mitigation [8].

In most recent demonstrations where PSAs have been used for transmission or signal processing applications, the PSA has been realized using parametric gain in either highly nonlinear fibers (HNLFs) [9, 10], or periodically poled lithium niobate (PPLN) waveguides [11, 12]. For applications where low-noise amplification is desired HNLF-based implementations are preferred since PPLN-based implementations suffer from high insertion loss which directly impact the noise figure (NF). Using HNLF to implement a fiber optical parametric amplifier (FOPA) phase-sensitive (PS) parametric gain is obtained through four-wave mixing (FWM). The FWM process involves interaction between one or two pump waves, a signal wave, and an idler wave. Depending on how the frequencies of the interacting waves are chosen, different amplification schemes can be realized [13].

The simplest scheme allowing for low-noise amplification and modulation format independent nonlinearity mitigation is the so-called degenerate pump two-mode PSA. In theory, when compared at the same signal gain, two-mode PSAs add 6 dB less noise than PIAs, such as EDFAs [1]. An alternative way to express this is that with the same output noise power two-mode PSAs will provide 6 dB higher signal gain than PIAs. The reduction in amplifier noise using PSAs can in single-span systems enable improved sensitivity by 6 dB [2, 4], and in multi-span systems operating in a linear transmission regime allow for a fourfold increase in the number of transmission spans, and thus also a fourfold increase in transmission reach [8, 14].

In addition to the benefit gained from low-noise amplification, two-mode PSAs also allow for larger accumulated nonlinear phase shifts than PIAs, through the mitigation of nonlinear transmission distortions. In single-span systems this can enable increased launch power tolerance [4], and in multi-span systems operating in a nonlinear transmission regime it can allow for an increased number of transmission spans [8]. The increased nonlinear phase shift tolerance is determined by the kind of nonlinear distortions that can be mitigated and how efficient the mitigation is. It should be noted that when using two-mode PSAs, two signal-carrying waves are transmitted over the system. The improvement from low-noise amplification and nonlinearity mitigation thus come at the cost of reduced spectral efficiency (SE) by a factor of two.

In the nonlinear transmission regime various nonlinear transmission distortions will degrade the signal. The fiber nonlinearities can be classified as intra-channel effects and inter-channel effects [5]. Intra-channel effects can further be divided into nonlinear signal-signal interaction which results in self-phase modulation (SPM), and nonlinear signal-noise interaction resulting in nonlinear phase noise (NLPN). The nonlinear signal-noise interaction is sometimes referred to as the Gordon-Mollenauer effect [15]. The inter-channel effects, present only in wavelength division multiplexing (WDM) systems, give rise to cross-phase modulation (XPM) and FWM through nonlinear signal-signal interaction and NLPN through nonlinear signal-noise interaction. Which ones of these nonlinear effects that will dominate the signal distortion depends on the design and parameters of the particular transmission system.

In well-designed single-span transmission systems no NLPN is generated since the optical signal-to-noise ratio (OSNR) of the signal launched into the transmission span is high. In single-span single-channel systems the signal distortion from nonlinearities will therefore be dominated by SPM. Most of the previous experimental investigations of nonlinearity mitigation in PSA-amplified systems have focused on the single-span single-channel case, where the increased launch power tolerance is obtained solely from mitigation of SPM-induced distortions.

#235784 - $15.00 USD Received 6 Mar 2015; revised 15 Apr 2015; accepted 16 Apr 2015; published 24 Apr 2015

In this type of system increased launch power tolerances of 3 dB have been reported transmitting quadrature phase-shift keying (QPSK) data [16], and 6 dB transmitting 16-ary quadrature amplitude modulation (16QAM) data [4].

In multi-span transmission systems each in-line amplifier will add noise to the signal and the OSNR will successively degrade throughout the system. Due to the accumulation of amplifier noise a significant amount of NLPN can be generated through nonlinear signal-noise interaction. It has been shown that in dispersion managed PIA-amplified multi-span systems transmitting single-channel QPSK data, NLPN will dominate the nonlinear signal distortion at symbol rates below 40 GBd while SPM will dominate at higher symbol rates [17]. It has not been investigated what nonlinear distortions will dominate in single-channel PSA-amplified systems, but since they require span-wise dispersion compensation with no residual dispersion [10], and thus are similar to dispersion managed systems, it is reasonable to assume that NLPN will also be important in single-channel PSA-amplified systems. Furthermore, with SPM-induced distortions already mitigated, NLPN might become the dominant impairment in systems where it would normally not be an issue.

In the recent demonstration of PSA-amplified multi-span transmission [8], an increased transmission reach compared to a conventional PIA-amplified system was demonstrated also when operating in a strongly nonlinear regime, where both SPM- and NLPN-induced distortions degrade the signal. Most likely, both SPM mitigation and NLPN mitigation in the PSA-amplified system enabled the transmission reach increase. However, it was not explicitly shown that NLPN mitigation took place since SPM mitigation and possible NLPN mitigation could not be distinguished. The only previous demonstration of NLPN mitigation in PSA-amplified systems was based on numerical simulations [4].

In this paper we present the first experimental demonstration of NLPN mitigation in PSA-amplified transmission systems. We study a single-span system with noise loading in the transmitter to obtain significant nonlinear signal-noise interaction in the transmission span and in that way emulate the conditions in a multi-span system. By considering not only the case of correlated noise on the signal and idler waves at the transmission span input, which is the situation in PSA-amplified transmission systems, but also the case of uncorrelated noise on the two waves we can clearly illustrate the NLPN mitigation. To provide a more complete understanding of the impact of in-line amplifier noise in PSA-amplified transmission systems we discuss the case of linear propagation in addition to the case of nonlinear propagation, in which NLPN is generated. To complement the experimental demonstration we also present numerical simulations which show excellent agreement with the experiments.

The paper is organized as follows. In Section 2 we discuss the impact of in-line amplifier noise in PSA-amplified transmission systems, considering both linear and nonlinear propagation in the transmission span. In Section 3 we present the numerical model used for the simulations and the simulation results. In Section 4 the experimental demonstration is presented. In Section 5 we discuss the results and finally in Section 6 we conclude the paper.

2. In-line amplifier noise in PSA-amplified systems

In a simplified description the noise at a given point in a transmission system can be assumed to constitute of vacuum noise and excess noise. Vacuum noise is always present and has a constant noise power while excess noise is introduced by in-line amplifiers and increase in power with each amplifier. With ideal amplification the noise introduced by an amplifier corresponds to the amplification of the vacuum noise present at its input. In a transmission system the signal degradation due to excess noise depend on the type of amplifiers used and the strength of the fiber nonlinearities in the transmission span. We will discuss the cases of linear propagation and strongly nonlinear propagation and compare degenerate pump two-mode PSAs, capable of

#235784 - $15.00 USD Received 6 Mar 2015; revised 15 Apr 2015; accepted 16 Apr 2015; published 24 Apr 2015

low-noise amplification and nonlinearity mitigation, to conventional PIAs.

2.1. Linear propagation

When propagating a signal accompanied by excess noise in a multi-span system operating in the linear regime the propagation itself will not result in any noise-related degradation, such as NLPN in the nonlinear regime. Noise-related degradation will only occur when more noise is added to the signal at in-line amplifiers. When using PSAs as in-line amplifiers a fourfold transmission reach improvement can be obtained, compared to when using PIAs, due to low-noise amplification.

In multi-span systems each in-line amplifier will alter the OSNR. The degree of change depends on the amount of excess noise present at the amplifier input and the amount of noise added by the amplifier. Without any excess noise present at the input, i.e. with a shot noise limited input signal, a PSA will improve the OSNR by 3 dB (taking into account only the signal wave power at the input) while a PIA will degrade the OSNR by 3 dB.

To help us understand the numerical and experimental results, where we consider cases with different amount of excess noise present at the amplifier input, we will study the impact of excess noise on the difference in OSNR change between PSA- and PIA-amplification. To this end we will analyze a single amplifier using a simple analytical model.

A degenerate pump two-mode FOPA PSA without pump depletion can be described by the transfer matrix equation [18]

$$\begin{bmatrix} B_{\mathrm{s}} \\ B_{\mathrm{i}}^{*} \end{bmatrix} = \begin{bmatrix} \mu & \nu \\ \nu^{*} & \mu^{*} \end{bmatrix} \begin{bmatrix} A_{\mathrm{s}} + n_{\mathrm{exc,s}} + n_{\mathrm{vac,s}} \\ A_{\mathrm{i}}^{*} + n_{\mathrm{exc,i}}^{*} + n_{\mathrm{vac,i}}^{*} \end{bmatrix}, \tag{1}$$

where A represent the input wave amplitudes, B represent the output wave amplitudes, μ and ν are complex transfer coefficients, n_{exc} represent the input excess noise, n_{vac} represent the input vacuum noise, subscript s denote the signal and i denote the idler, and superscript $*$ denote the complex conjugate operation. The complex transfer coefficients satisfy the relation $|\mu|^2 - |\nu|^2 = 1$ which implies that the signal and idler waves are amplified. In a semi-classical description, which we consider here, the vacuum noise is described by Gaussian noise (GN) that satisfies $\langle n_m \rangle = 0$, $\langle n_m n_l \rangle = 0$, and $\langle |n_m|^2 \rangle = \hbar\omega_m/2$ with $m,l \in \{\mathrm{s},\mathrm{i}\}$ [19], where $\langle . \rangle$ denotes a statistical average. For readability we express the output wave amplitudes B as

$$B_{\mathrm{s}} = \mu A_{\mathrm{s}} + \nu A_{\mathrm{i}}^{*} + \mu n_{\mathrm{exc,s}} + \nu n_{\mathrm{exc,i}}^{*} + \mu n_{\mathrm{vac,s}} + \nu n_{\mathrm{vac,i}}^{*} \tag{2}$$

and

$$B_{\mathrm{i}} = \nu A_{\mathrm{s}}^{*} + \mu A_{\mathrm{i}} + \nu n_{\mathrm{exc,s}}^{*} + \mu n_{\mathrm{exc,i}} + \nu n_{\mathrm{vac,s}}^{*} + \mu n_{\mathrm{vac,i}}. \tag{3}$$

The OSNR change caused by a PSA is determined not only by the amount of excess noise present at the amplifier input but also the relation between the noise on the signal and idler waves. An important distinction can be made between having correlated or uncorrelated noise on the two waves, where correlated noise will add coherently in the PSA while uncorrelated noise will add incoherently. The vacuum noise on the signal and idler waves is always uncorrelated and will therefore always add incoherently. The excess noise on the other hand can, in principle, be either correlated or uncorrelated.

In a PSA-amplified transmission system the excess noise at the output of each PSA will be correlated and conjugated on the two waves, which can be seen by studying (2) and (3) in the high-gain regime, i.e. $|\mu| \approx |\nu|$. If this condition is maintained over the transmission span the excess noise will add coherently in the following PSA. The conjugation of the noise is important since that will lead to amplification of both quadratures, as opposed to amplification of one quadrature and de-amplification of the other quadrature which is the case with correlated but un-conjugated noise [9].

#235784 - $15.00 USD Received 6 Mar 2015; revised 15 Apr 2015; accepted 16 Apr 2015; published 24 Apr 2015

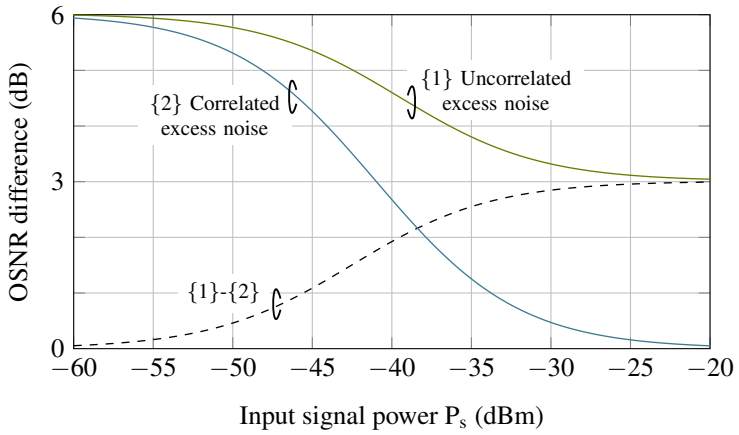

Fig. 1. Output OSNR difference between PSA-amplification, with correlated or uncorrelated excess noise at the amplifier input, and PIA-amplification versus input signal power with 20 dB input OSNR. The dashed line represents the difference between the case of having uncorrelated and correlated excess noise.

The presence of excess noise at the amplifier input will reduce the 6 dB OSNR difference between PSA- and PIA-amplification that was obtained with a shot noise limited input signal. This has been shown in the case of having uncorrelated noise on the two waves [20, 21]. To obtain quantitative results for the impact of excess noise on the difference in OSNR change between PSA- and PIA-amplification we will calculate the output OSNR difference between PSA- and PIA-amplification versus signal input power for a given input OSNR, both with correlated and uncorrelated excess noise.

A FOPA PIA can be described by (1) if we set $A_\mathrm{i} = 0$ and $n_\mathrm{exc,i} = 0$. The output OSNR can in the limit of high gain can be expressed as $\mathrm{OSNR}_\mathrm{PIA} = P_\mathrm{s}/(P_\mathrm{exc} + 2P_\mathrm{vac})$ [20], where $P_\mathrm{s} = |A_\mathrm{s}|^2$ is the input signal power, P_exc the input excess noise power, and P_vac the vacuum noise power, with the value -61 dBm taken over a bandwidth of 0.1 nm at the center wavelength of 1550 nm [20]. The output OSNR for a PSA with input excess noise that is uncorrelated can be expressed as $\mathrm{OSNR}_\mathrm{PSA,uc} = 4P_\mathrm{s}/(2P_\mathrm{exc} + 2P_\mathrm{vac})$ [20]. The factor of four before P_s originates from the coherent addition of signal and idler waves and the factor of two before P_exc from the incoherent addition of the excess noise on the signal and idler waves. Following the same approach the output OSNR for a PSA with correlated input excess noise can be expressed as $\mathrm{OSNR}_\mathrm{PSA,c} = 4P_\mathrm{s}/(4P_\mathrm{exc} + 2P_\mathrm{vac})$. The output OSNR difference between PSA- and PIA-amplification can now respectively, for the case of correlated and uncorrelated excess noise, be expressed as

$$\frac{\mathrm{OSNR}_\mathrm{PSA,c}}{\mathrm{OSNR}_\mathrm{PIA}} = \frac{4 + 2P_\mathrm{exc}/P_\mathrm{vac}}{1 + 2P_\mathrm{exc}/P_\mathrm{vac}} \quad \text{and} \quad \frac{\mathrm{OSNR}_\mathrm{PSA,uc}}{\mathrm{OSNR}_\mathrm{PIA}} = \frac{4 + 2P_\mathrm{exc}/P_\mathrm{vac}}{1 + P_\mathrm{exc}/P_\mathrm{vac}}. \tag{4}$$

By writing the excess noise power as $P_\mathrm{exc} = P_\mathrm{s}/\mathrm{OSNR}_\mathrm{in}$, where $\mathrm{OSNR}_\mathrm{in}$ represent the OSNR at the amplifier input, we can plot the output OSNR differences versus input signal power for a given input OSNR. In Fig. 1 we present curves corresponding to an input OSNR of 20 dB. At low input signal powers the OSNR difference is the same in both cases which is expected since the excess noise is negligible compared to the vacuum noise. The 6 dB difference between PSA-amplification and PIA-amplification is due to the coherent addition of the signal and idler waves in the PSA, resulting in 6 dB higher signal gain, while the amount of vacuum noise coupled to the signal is the same in both cases. At high input signal powers the excess noise is

#235784 - $15.00 USD Received 6 Mar 2015; revised 15 Apr 2015; accepted 16 Apr 2015; published 24 Apr 2015

dominating and the OSNR difference is 0 dB for the case with correlated excess noise and 3 dB for the case with uncorrelated excess noise. With correlated excess noise both the signal and the excess noise will experience the same gain in the PSA, as is the case for PIA-amplification, while with uncorrelated excess noise the signal will experience 3 dB higher gain than the excess noise. The dashed line in Fig. 1 represent the difference between the case of having uncorrelated and correlated excess noise.

2.2. Nonlinear propagation

In the case of nonlinear propagation the presence of excess noise will lead to generation of NLPN though nonlinear signal-noise interaction. This will impact the signal wave by changing the distribution of the excess noise from Gaussian to non-Gaussian [22]. With non-Gaussian excess noise accompanying the signal wave its quality cannot reliably be assessed using the OSNR and an analytical description of the system is not straightforward. In this section we will briefly qualitatively discuss the difference between PSA- and PIA-amplification while a quantitative comparison will be provided by the numerical and experimental results presented in Section 3 and Section 4.

Amplification of a signal degraded by NLPN using a PIA will only affect the signal by the addition of amplifier noise. Using a PSA, amplifier noise will also be added to the signal but in this case the amplifier can also affect the distribution of the excess noise through the addition of the excess noise on the signal and idler waves. The addition carried out by the PSA, illustrated by (2), can re-distribute the excess noise present at the amplifier input in such a way that the phase noise is reduced. This will reduce the impact of the NLPN and improve the signal quality, particularly when transmitting phase modulated data.

The principle for mitigation of NLPN is analogous to the principle for SPM mitigation presented in [4]. The signal and idler waves, having correlated and conjugated excess noise at the input of the transmission span, will experience similar nonlinear phase rotation, given that the dispersion map is optimized [4, 16]. In the following PSA the NLPN on the two waves will be modified by phase to amplitude conversion, analogous to the phase to amplitude conversion observed in the case of SPM mitigation [4]. The distribution of the NLPN will change also if the excess noise at the transmission span input is uncorrelated. However, the reduction in phase noise will only be marginal compared to the case of having correlated excess noise.

3. Numerical simulations

To illustrate and investigate the NLPN mitigation in PSA-amplified transmission systems using numerical simulations we modeled a single-span single-channel system with noise loading in the transmitter. The PSA was placed as preamplifier after the transmission span and we studied the cases of having either correlated or uncorrelated excess noise on the signal and idler waves at the input of the transmission span. We also simulated an ordinary PIA-amplified system as a benchmark.

3.1. Simulation models

The model used for the PIA-amplified system is illustrated in Fig. 2 and the model used for the PSA-amplified system is illustrated in Fig. 3. In both systems we generated a single-polarization 10 GBd QPSK non-return-to-zero (NRZ) signal using an IQ modulator with 28 GHz bandwidth (emulated by a Gaussian filter). The signal contained 2^{20} symbols of random data with 16 samples per symbol. In the PSA-amplified system an idler wave was generated by copying and conjugating the signal wave. In both systems noise loading was performed in the transmitter by adding GN. In the PSA-amplified system the noise was added before generating the idler wave

#235784 - $15.00 USD Received 6 Mar 2015; revised 15 Apr 2015; accepted 16 Apr 2015; published 24 Apr 2015

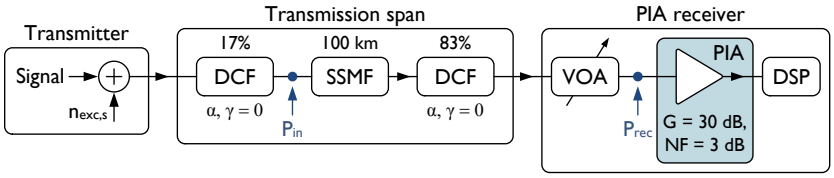

Fig. 2. Simulation model for a PIA-amplified transmission system. Acronyms are explained in the text.

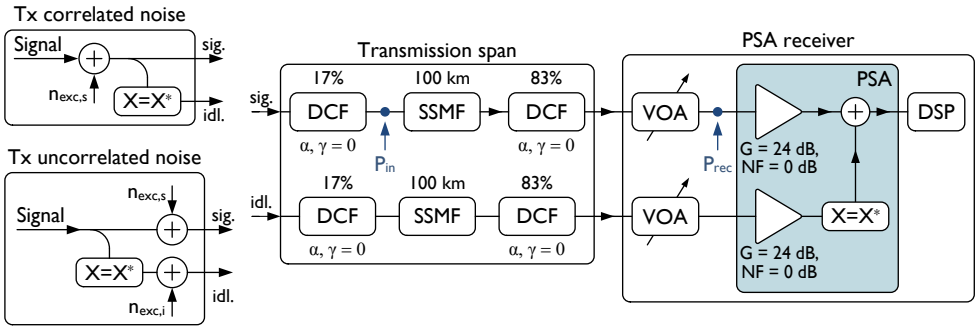

Fig. 3. Simulation model for a PSA-amplified transmission system with either correlated or uncorrelated excess noise on the signal and idler waves at the transmission span input. Acronyms are explained in the text.

to obtain the case of correlated noise and after generating the idler wave to obtain the case of uncorrelated noise.

The transmission span consisted of 100 km standard single mode fiber (SSMF) with dispersion compensating fiber (DCF) for dispersion compensation. Propagation in the SSMF was modeled by solving a single-polarization nonlinear Schrödinger equation (NLSE) using the split-step Fourier method (SSFM) and the SSMF parameters were $\alpha = 0.25$ dB/km, $\beta_2 = 17.4$ ps/(nm km), and $\gamma = 1.5$ (W km)$^{-1}$. Raman scattering and higher-order dispersion were neglected. Dispersion compensation was done in a single step neglecting both attenuation and nonlinearity in the DCF. The transmission span had a dispersion map with 17% pre-compensation and 83% post-compensation. Simulations (not presented here) with high launch powers into the transmission span and without noise added in the receiver showed that this dispersion map was optimal in terms of the improvement gained from nonlinearity mitigation when comparing the PSA-amplified system with correlated noise to the PIA-amplified system. The optimal dispersion map was the same (17% pre-compensation and 83% post-compensation) both with 20 dB OSNR at the transmission span input, resulting in a nonlinear degradation dominated by NLPN, and with 50 dB OSNR at the transmission span input, resulting in a nonlinear degradation dominated by SPM. Furthermore, the penalty caused by deviating from the optimal dispersion was similar both with 20 dB OSNR and 50 dB OSNR, indicating that dispersion map optimization is of similar importance for SPM mitigation [4], and NLPN mitigation. The dispersion map was also optimal in terms of the absolute performance for the PSA-amplified system with correlated noise.

The simulations were performed to complement the experiments presented in Section 4. In the experiments the signal and idler waves were separated by 8 nm, resulting in negligible nonlinear interaction (XPM and FWM) between the two waves due to large walk off. As a result of the negligible nonlinear interaction between the waves we could use a simplified simulation

#235784 - $15.00 USD Received 6 Mar 2015; revised 15 Apr 2015; accepted 16 Apr 2015; published 24 Apr 2015

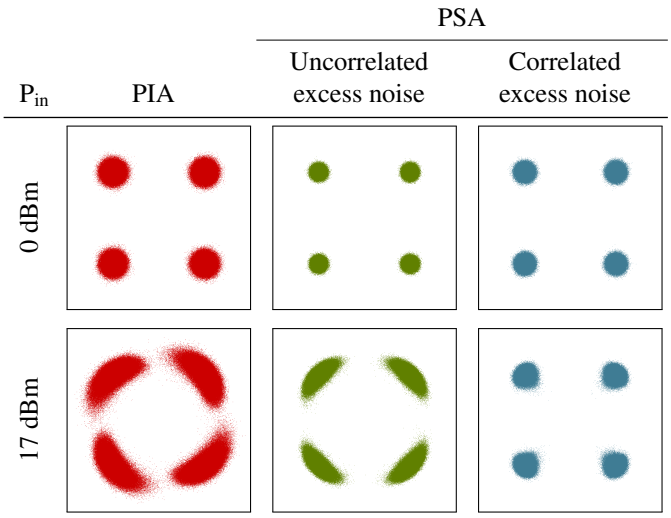

Fig. 4. Simulated signal wave constellation diagrams with −37 dBm received power and 20 dB OSNR at the transmission span input.

model for the PSA-amplified transmission system where the signal and idler waves were propagated individually in two different fibers. The same fiber parameters were used both for signal wave and idler wave propagation. The span launch power was determined at point P_{in}.

In the PIA-amplified system the receiver consisted of a variable optical attenuator (VOA), a PIA, and a digital signal processing (DSP) block. The VOA was used to vary the received power while keeping the transmission span unchanged. The PIA was modeled by a single block with 30 dB gain and 3 dB NF. This could e.g. represent amplification by an ideal EDFA. The receiver in the PSA-amplified system consisted of two VOAs, a PSA, and a DSP block. The PSA was modeled by first amplifying the signal and idler waves individually using an amplifier with 24 dB gain and 0 dB NF and then conjugating the idler wave and adding it to the signal wave. These operations are analogous to what a PSA does in the high-gain regime. The net signal PSA gain was 30 dB, thus the same as for the PIA, and the signal NF was −3 dB when only accounting for the signal wave power at the PSA input [13], or 0 dB when accounting for both the signal wave power and the idler wave power. The idler wave phase was rotated before being added to the signal wave to maximize the optical power after addition, emulating the operation of the phase-locked loop (PLL) in an experimental system [23]. This phase adjustment was constant over all simulated symbols, mimicking the slow (kHz) response of the PLL. We used conventional DSP for post-processing of the QPSK signal, the same in both the PSA- and the PIA-amplified system. The received power was determined at point P_{rec}.

3.2. Simulation results

To first get a qualitative understanding of the nonlinearity mitigation we will study constellation diagrams of the signal wave after amplification at high received power, where the nonlinear distortion is clearly visible. In Fig. 4 we compare the PIA-amplified system to the PSA-amplified systems at 0 dBm and 17 dBm launch power, with −37 dBm received power and 20 dB OSNR at the transmission span input. At 0 dBm launch power the signal wave experience no nonlinear distortion and the only difference between the three systems is the amount of noise on the signal wave. The PSA-amplified systems provide better OSNR than the PIA-amplified system and the PSA-amplified system with uncorrelated excess noise provide better OSNR than the

#235784 - $15.00 USD Received 6 Mar 2015; revised 15 Apr 2015; accepted 16 Apr 2015; published 24 Apr 2015

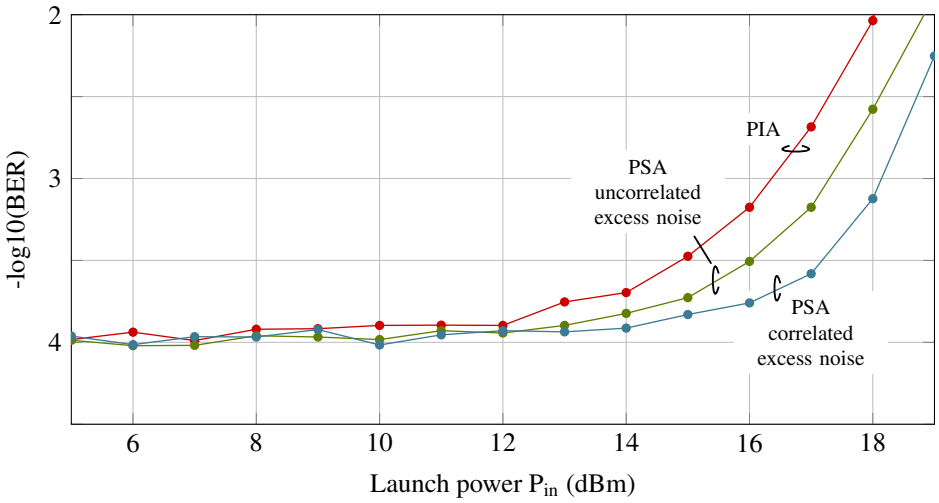

Fig. 5. Simulated BER versus launch power with the received power kept fixed at a value giving a BER of about 1×10^{-4} at 0 dB launch power. The OSNR at the transmission span input was 20 dB.

PSA-amplified system with correlated excess noise. This is also what we expect from Fig. 1. At 17 dBm launch power the propagation is nonlinear which is seen from the phase rotation and increased phase noise in the PIA-amplified system. The PSA-amplified system with uncorrelated noise show a clear improvement compared to the PIA-amplified system which is attributed to improved noise performance due to low-noise amplification and incoherent addition of excess noise, mitigation of SPM-induced distortions, and re-distribution of NLPN. The impact of NLPN re-distribution is only marginal since the excess noise is uncorrelated. Considering the case of correlated noise we see further reduction in phase noise which is explained by NLPN mitigation. The increase in amplitude noise for this case is due to the phase to amplitude conversion in the PSA [4]. The nonlinear phase shift in the two cases can be calculated from $\phi_{\mathrm{NL}} = \gamma P L_{\mathrm{eff}}$, where P is the launch power, L_{eff} the effective length defined as $L_{\mathrm{eff}} = [1-\exp(-\alpha L)]/\alpha$ with α being the fiber attenuation, and L the span length. In the 0 dB case it was 0.03 rad and in the 17 dBm case 1.30 rad.

To obtain a quantitative measure of the benefit gained from the nonlinearity mitigation the bit error ratio (BER) versus launch power was calculated and is presented in Fig. 5. The received power was in each system adjusted to get a BER of about 1×10^{-4} at 0 dBm launch power and then, while keeping the received power constant by adjusting the VOA, the launch power was increased. In the PIA-amplified system the received power giving a BER of about 1×10^{-4} was -46.8 dBm, in the PSA-amplified system with uncorrelated noise -52.9 dBm, and in the PSA-amplified system with correlated noise -52.8 dBm. We note that the 0.1 dB power difference between the PSA-amplified system with correlated noise and the PSA-amplified system with uncorrelated noise corresponds roughly to the 0.25 dB difference that is expected from Fig. 1. The differences seen between the three cases in Fig. 5 are only due to nonlinearity mitigation since the amount of excess noise on the signal wave is the same in all cases. In the PIA-amplified system there is no mitigation of nonlinearities while in the PSA-amplified system with uncorrelated noise mainly SPM-induced distortions are mitigation and in the PSA-amplified system with correlated noise both SPM-induced distortions and NLPN is mitigated. The penalty seen at high launch powers in the PSA-amplified system with correlated noise is

#235784 - $15.00 USD Received 6 Mar 2015; revised 15 Apr 2015; accepted 16 Apr 2015; published 24 Apr 2015

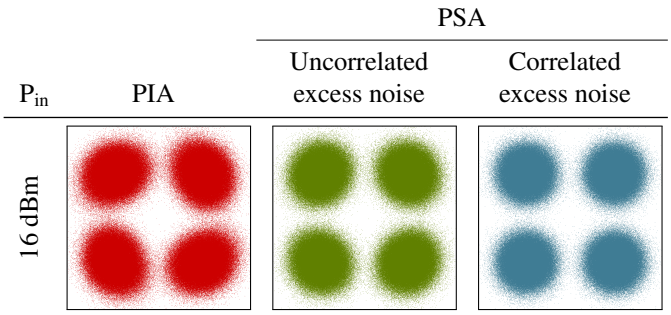

Fig. 6. Simulated signal wave constellation diagrams corresponding to the 16 dBm launch power point in Fig. 5.

due to amplitude noise introduced by the phase to amplitude conversion in the PSA.

Constellation diagrams of the signal wave after amplification corresponding to the 16 dBm launch power point in Fig. 5 are presented in Fig. 6. The difference in nonlinearity mitigation between the three systems can be distinguished but is not as clear as in Fig. 4 due to the presence of more amplifier noise.

4. Experimental demonstration

To experimentally demonstrate and investigate the NLPN mitigation in PSA-amplified systems we carried out a single-span single-channel transmission experiment with noise loading giving either correlated or uncorrelated excess noise on the signal and idler waves at the transmission span input. We compared the operation of a PSA-amplified system both with a PIA-amplified system and an EDFA-amplified system. The PSA and PIA were implemented using a FOPA.

4.1. Experimental setup

The experimental setup is illustrated in Fig. 7 and was based on previous demonstrations [4, 16, 23]. A 10 GBd QPSK signal at 1549.5 nm was combined with a 28 dBm continuous wave (CW) pump at 1553.7 nm using a WDM coupler. The waves were launched into the copier which consisted of two cascaded spools of HNLF with an isolator in between for suppression of stimulated Brillouin scattering (SBS). An idler wave at 1557.5 nm was generated in the copier through FWM with a net conversion efficiency of about -5 dBm. Polarization controllers (PCs) in the signal wave and pump wave paths were used to maximize the copier gain. After the copier the pump wave was separated from the signal and idler waves and attenuated for 2 dBm launch power into the SSMF using a VOA and then passed through an optical delay line for equalization of the optical path covered by the pump wave and the signal and idler waves between the copier and the PSA. Since no phase-dithering was applied to the pump wave for SBS suppression a rough path equalization was sufficient. The signal and idler waves were passed through an optical processor for amplitude and delay adjustments. The signal and idler wave amplitudes were balanced and the relative delay between the waves was adjusted to minimize the delay difference at the PSA input. The optical processor was also used for switching between phase-insensitive (PI) and PS operation by either blocking or letting through the idler wave.

A noise loading stage consisting of a polarized amplified spontaneous emission (ASE) source, an optical processor, and a PC was used to generate noise with a specific spectral power profile and polarization. To obtain correlated excess noise on the signal and idler waves ASE noise was coupled to the signal wave before the copier. The noise power was adjusted to get

#235784 - $15.00 USD Received 6 Mar 2015; revised 15 Apr 2015; accepted 16 Apr 2015; published 24 Apr 2015

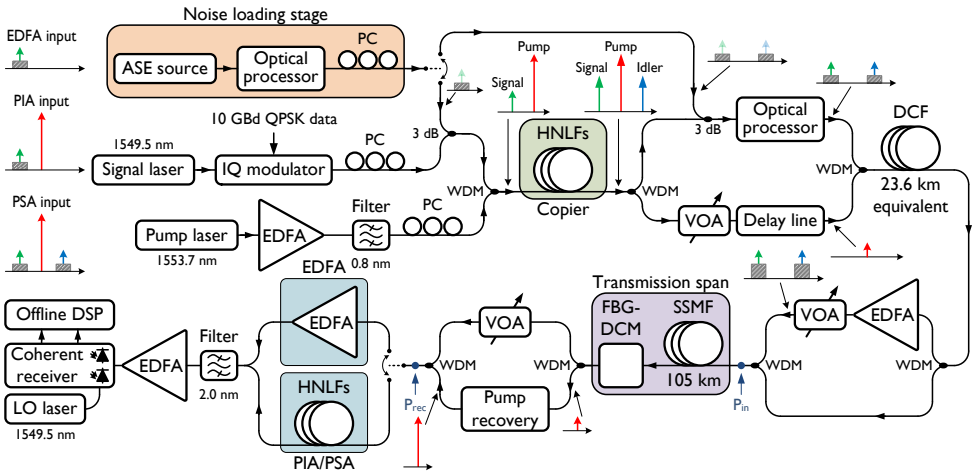

Fig. 7. Experimental setup used for demonstrating and investigating NLPN mitigation in PSA-amplified transmission systems. Acronyms are explained in the text.

an OSNR of 20 dB and the PC in the noise loading stage was adjusted so that the ASE was co-polarized with the signal wave. The idler wave generated in the copier had the same OSNR as the signal wave. To obtain uncorrelated excess noise on the signal and idler waves ASE noise was instead coupled to the signal and idler waves individually after the copier. The polarization of the noise was aligned with the polarization of the signal and idler waves and the noise power in the signal wave and idler wave bands were set so that both waves obtained an OSNR of 20 dB.

After the three waves were re-combined they were launched into a DCF for pre-compensation equivalent to 23.6 km of SSMF. The signal wave and idler wave powers launched into the DCF were about -10 dBm and the pump wave power was about 5 dBm. After the DCF the pump wave was again separated from the signal and idler waves and led unaffected through one branch while the signal and idler waves were amplified by an EDFA and then attenuated by a VOA to set the desired launch power into the transmission span. The launch power was measured at point P_{in} indicated in Fig. 7. The transmission span consisted of 105 km SSMF followed by a fiber Bragg-grating dispersion-compensating module (FBG-DCM) compensating for the remainder of the dispersion. The dispersion map was chosen based on an optimum for efficient nonlinearity mitigation found for 10 GBd QPSK data [16].

After the transmission span the signal and idler waves were passed through a VOA to vary the received power, measured at point P_{rec} as indicated in Fig. 7. Only the signal wave power was included for when measuring launch power and received power. The pump wave was re-generated and amplified to 30 dBm using a hybrid EDFA/injection-locking system [23], and then launched into the PIA/PSA together with the signal and idler waves. The pump recovery stage included a PLL to lock the relative phase between the pump wave and the signal and idler waves for maximum gain in the PSA [23]. The phase instability resulting in gain drift was introduced by thermal drift and acoustic noise caused by splitting the pump wave and the signal and idler waves in different paths. The PIA/PSA FOPA was implemented with a cascade of four HNLFs similar to the one described in [24], and provided 20.8 dB net gain in PS-mode and 15.0 dB net gain in PI-mode.

The amplified signal was then filtered and passed to a preamplified coherent receiver where it was mixed with a 300 kHz linewidth local oscillator (LO) laser at 1549.5 nm in a 90° hybrid

#235784 - $15.00 USD Received 6 Mar 2015; revised 15 Apr 2015; accepted 16 Apr 2015; published 24 Apr 2015

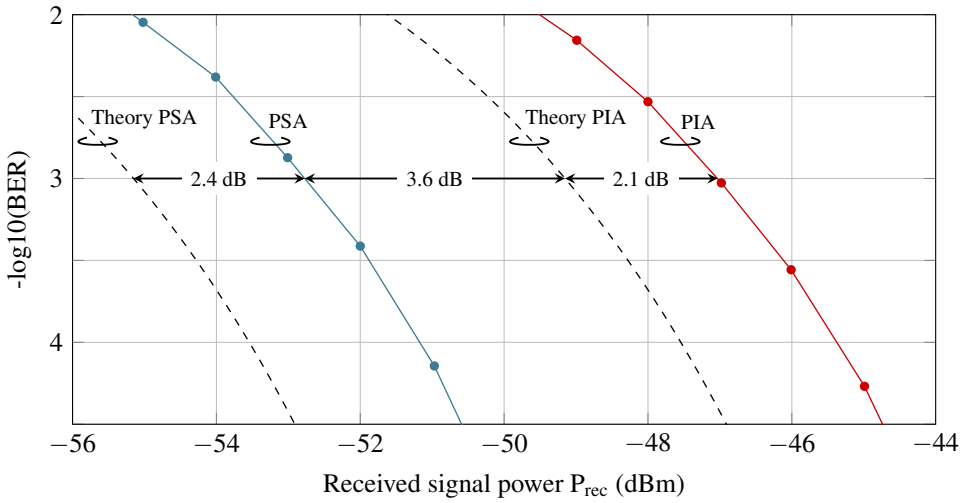

Fig. 8. Comparison of experimentally measured B2B sensitivity for the PIA- and PSA-amplified systems with corresponding analytical curves.

followed by detection and sampling using balanced photodiodes and a real-time sampling oscilloscope with 16 GHz bandwidth. The DSP in the receiver was conventional DSP for QPSK. The spectra in Fig. 7 illustrate the case of PSA-amplification with uncorrelated excess noise on the signal and idler waves.

4.2. Experimental results

To characterize the transmitter and the preamplifier FOPA we carried out measurements of the back-to-back (B2B) sensitivity, which are presented in Fig. 8. The B2B system was obtained by disconnecting the noise loading stage and connecting the output of the WDM coupler before the DCF to the input of the WDM coupler after the transmission span. In Fig. 8 we have also included theoretical B2B curves representing ideal PIA- and PSA-amplification. The theoretical curve for PIA-amplification was calculated from BER $= \mathrm{erfc}[\sqrt{P_{\mathrm{rec}}/(hfB)}]/2$ [25], where P_{rec} represent the received power, hf the photon energy, and B the bit rate. The theoretical curve for PSA-amplification was obtained by shifting the PIA-curve by 6 dB.

The implementation penalty for the PIA-amplified system was 2.1 dB and the PSA-amplified system provided a sensitivity of -52.8 dBm at a BER of 1×10^{-3} which corresponds to 2.0 photons per bit. Accounting for the power of both the signal wave and the idler wave the sensitivity was -49.8 dBm, or 4.1 photons per bit. The theoretical sensitivity limit for a PIA-amplified system at a BER of 1×10^{-3} is -49.2 dBm, or 4.7 photons per bit. The PSA-amplified system thus provided 0.6 dB better sensitivity than the theoretical limit for PIA-amplified systems and, to the best of our knowledge, the highest sensitivity ever demonstrated for QPSK.

Measured BER versus received power for the complete transmission system with 0 dBm launch power, corresponding to linear propagation, and 20 dB OSNR at the transmission span input is presented in Fig. 9. Comparing with Fig. 8 we see that the noise loading and the presence of the transmission span had very small impact when transmitting in the linear regime. The growing difference with increased received power between the two PSA-amplified systems is attributed to the increasing impact of excess noise. This is also what we expect from the analytical model and Fig. 1. We also note that the difference between the PIA and the PSA case is close to the theoretical 6 dB which indicates that the PSA was operating well. The FOPA PIA

#235784 - $15.00 USD Received 6 Mar 2015; revised 15 Apr 2015; accepted 16 Apr 2015; published 24 Apr 2015

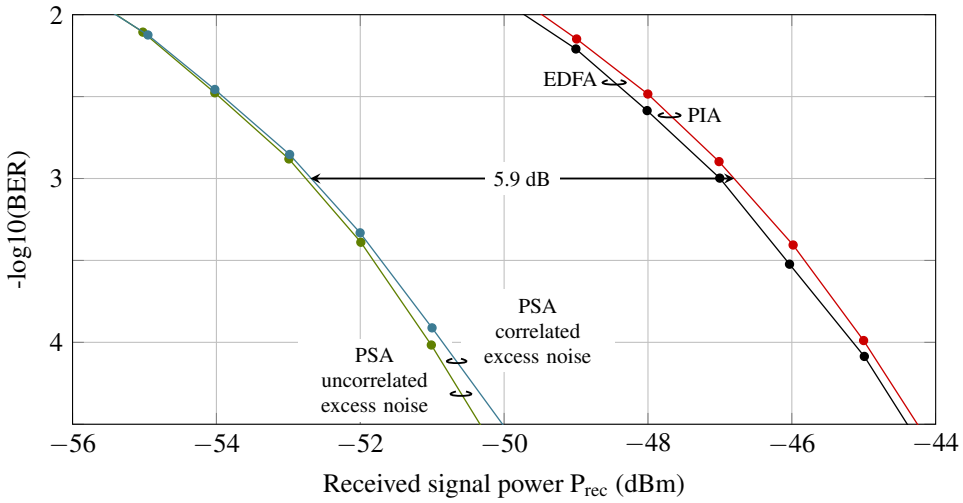

Fig. 9. Measured BER versus received signal power with 20 dB OSNR at the transmission span input and 0 dBm launch power corresponding to linear propagation.

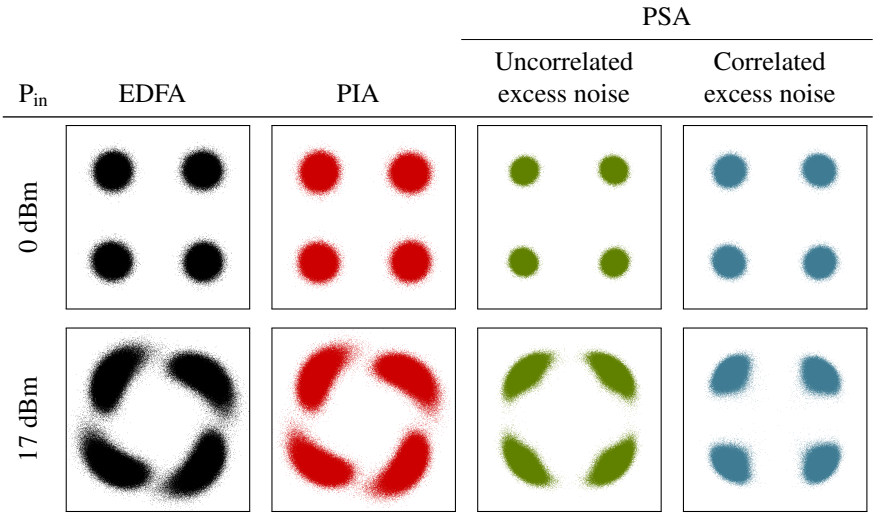

Fig. 10. Measured signal wave constellation diagrams with −37.0 dBm received power and 20 dB OSNR at the transmission span input.

and the EDFA show very similar performance which is anticipated since both are PIAs.

The following experimental results correspond to the same situations that were investigated numerically. Constellation diagrams of the signal wave after amplification for the four systems measured at −37 dBm received power and 20 dB OSNR at the transmission span input are presented in Fig. 10. Comparing with the numerical results presented in Fig. 4 we see that the qualitative features are similar with clearly visible SPM mitigation in the PSA-amplified system with uncorrelated excess noise and also NLPN mitigation in the PSA-amplified system with correlated excess noise. The EDFA-amplified system show the same qualitative features as the PIA-amplified system.

#235784 - $15.00 USD Received 6 Mar 2015; revised 15 Apr 2015; accepted 16 Apr 2015; published 24 Apr 2015

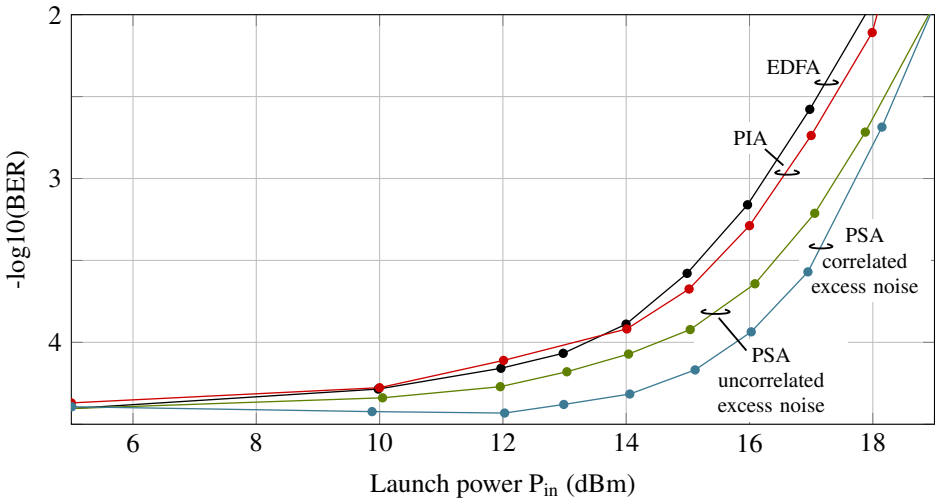

Fig. 11. Measured BER versus launch power with the received power kept fixed at a value giving a BER of 4×10^{-5} at 0 dBm launch power. The OSNR at the transmission span input was 20 dB.

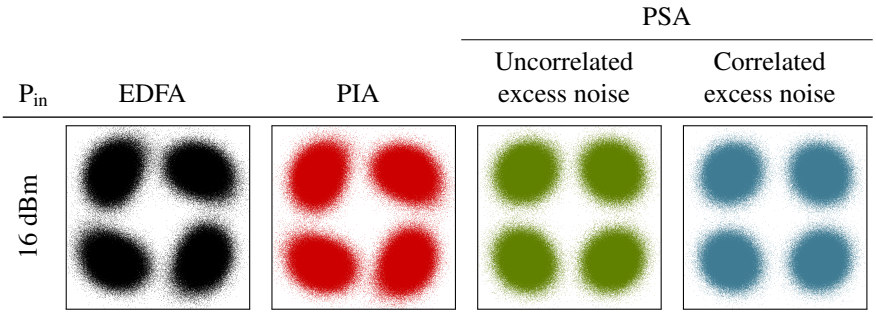

Fig. 12. Measured signal wave constellation diagrams corresponding to the 16 dBm launch power point in Fig. 11.

Measured BER versus launch power is presented in Fig. 11. The received power was in each system kept constant at a value giving a BER of about 4×10^{-5} at 0 dBm launch power and 20 dB OSNR at the transmission span input. For the EDFA-amplified system the received power was -44.4 dBm, for the PIA-amplified system -44.0 dBm, for the PSA-amplified system with uncorrelated noise -50.4 dBm, and for the PSA-amplified system with correlated noise -50.1 dBm. From Fig.1 we expect the power difference between the two PSA-amplified systems to be 0.45 dB which is in line with the 0.3 dB that we obtained experimentally. The interpretation of the results in Fig. 11 is the same as for the interpretation of the corresponding numerical results.

Constellation diagrams of the signal after amplification for the four systems corresponding to the 16 dBm launch power point in Fig. 11 are presented in Fig. 12. As for the numerical results the difference in nonlinearity mitigation between the three systems can be distinguished but is not as clear as in the case of -37 dBm received power due to more amplifier noise accompanying the signal.

#235784 - $15.00 USD Received 6 Mar 2015; revised 15 Apr 2015; accepted 16 Apr 2015; published 24 Apr 2015

5. Discussion

The demonstration of NLPN mitigation was carried out in a PSA-amplified single-span transmission system with noise loading in the transmitter. In a multi-span system NLPN would be introduced in each span and the NLPN mitigation would take place span-wise with each in-line PSA. Comparing a multi-span system with the single-span system we have studied we expect a smaller penalty from phase to amplitude conversion in the multi-span system for the same accumulated nonlinear phase shift. This is due to the span-wise nonlinearity mitigation and that the transfer function for the phase to amplitude conversion is not linear [4].

In addition to multi-span transmission it is also interesting to discuss the prospects of NLPN mitigation in multi-channel systems. Similar to how SPM mitigation is expected to work in multi-channel PSA-amplified transmission systems [4], we also expect NLPN mitigation to operate in such systems. The copier (in a single-span system) or the in-line PSAs (in a multi-span system) will ensure that a conjugated copy of the complete signal-band (including amplifier noise accompanying the signals) is present at the idler frequency at the input of the transmission span(s). With this condition fulfilled we expect that also inter-channel nonlinearities, including inter-channel signal-noise interaction, can be mitigated.

Apart from using PSAs several other techniques are also available to reduce the impact of fiber nonlinearities. A scheme closely related to the method presented in this paper is the phase-conjugated twin wave (PCTW) scheme. The principle to co-propagating two phase-conjugated is the same but the coherent addition is not performed all-optically in a PSA but in DSP after detecting the two waves using a coherent receiver [26, 27]. The PCTW scheme has proved capable of mitigating both intra- and inter-channel nonlinearities but is unable to efficiently mitigate NLPN since the excess noise on the two waves is uncorrelated, similarly to the PSA-amplified system with uncorrelated excess noise studied in this paper. Furthermore, the PCTW scheme is not compatible with span-wise mitigation.

Mid-span optical phase conjugation (OPC) is another scheme involving phase-conjugation [28]. As the name suggests the scheme relies on performing a phase-conjugating of the signal in the middle of the transmission system whereby nonlinear distortions introduced in the first half of the system will be reversed in the second half. With perfect dispersion and power symmetry over the system this scheme can in principle provide perfect compensation of intra- and inter-channel nonlinear signal-signal interaction and to some extent also mitigate nonlinear signal-noise interaction [29]. A scheme were multiple phase conjugations are performed along the link has also been demonstrated and this approach has shown improved performance compared to conventional mid-span OPC [30]. Another method for nonlinearity mitigation is digital backward propagation (DBP) which relies solely on DSP [31, 32]. DBP can compensate for all deterministic effects but not for non-deterministic effects such as NLPN.

6. Conclusion

We have presented the first experimental demonstration of NLPN mitigation in a modulation format independent PSA-amplified transmission system. It was shown that the NLPN mitigation is enabled by having correlated excess noise on the signal and idler waves at the input of the transmission span, which is always the case in PSA-amplified transmission systems. The experimental demonstration was complemented by numerical simulations showing excellent agreement with the experimental results. In addition to the demonstration of nonlinearity mitigation we also demonstrated a PSA-amplified receiver requiring 4.1 photons per bit (accounting for the power of both the signal and the idler waves) to obtain a BER of 1×10^{-3} with 10 GBd QPSK data. To the best of our knowledge this is the highest sensitivity ever reported for QPSK. The possibility to mitigate nonlinear transmission distortions, and in particular NLPN, along with low-noise amplification make PSAs unique and interesting for transmission system

#235784 - $15.00 USD Received 6 Mar 2015; revised 15 Apr 2015; accepted 16 Apr 2015; published 24 Apr 2015

applications.

Acknowledgments

This work was supported by the European Research Council Advanced Grant PSOPA (291618) and by the Knut and Alice Wallenberg Foundation. The authors would like to thank OFS Fitel Denmark for providing the HNLFs and acknowledge L. Liu for providing the code to the microcontroller-based PLL and A. Kumpera for assisting with implementing the PLL.

#235784 - $15.00 USD Received 6 Mar 2015; revised 15 Apr 2015; accepted 16 Apr 2015; published 24 Apr 2015